Supplemental Materials and Methods

Adolescent intermittent ethanol vapor exposure

Male Long-Evans rats were bred in house (Charles River breeding stock) and weaned at post-natal day 21. Rats were then divided into control and experimental groups and pair-housed in standard polycarbonate cages. Pairing was always done within litter and there was always a within litter control and experimental group (e.g., a litter size must have had a minimum of 4 male rats to be used in the study). Access to food and water in the home cage was continuous throughout the experiment.

The AIE exposure model used in the present study involved intermittent binge-like exposure to alcohol by vapor inhalation as previously described (Gass *et al.*, 2014). In brief, AIE exposure was carried out during early to middle adolescence (PD28-42) and involved 4 cycles of 2 consecutive episodes of exposure to alcohol vapor, with each exposure consisting of 14-hrs in the vapor chambers (a time period that encompassed the 12-hr lights-on sleep cycle) followed by 10-hrs out of the chambers during the dark cycle. Rats were exposed to alcohol on PD28 & 29 (cycle 1), PD32 & 33 (cycle 2), PD36 & 37 (cycle 3), and PD40 & 41 (cycle 4). A 5-point behavioral intoxication rating scale was used to provide an immediate index of the level of intoxication achieved during each of the exposure cycles (Gass *et al.*, 2014). We chose a target level of moderate intoxication, which corresponded to a rating of 2 to 3 on the intoxication scale. In addition to providing a measure of the level of intoxication, the rating also provided immediate information that could be used to make adjustments in the level of ethanol vapor in the chambers. Tail-vein blood was used to determine the BEC at the end of each of the 2-day ethanol vapor exposure cycles.

Dendritic spine imaging and 3D analysis

Diolistic labeling of slices obtained from fixed brains was used to assess the effects of AIE exposure on dendritic spine morphology in the PrL-C as previously described (Kroener *et al.*, 2012). In brief, adult (~PD90) AIE-exposed and control rats were anesthetized and perfused with 0.1 M phosphate buffer followed by 1.5% paraformaldehyde (PFA) in phosphate buffer and then post-fixed in 1.5% PFA for 60 min before coronal sections (150 μm) were prepared on a vibratome. Tungsten particles (1.3 μm diameter)

coated with DiI were delivered diolistically using a Helios Gene Gun (Bio-Rad) fitted with a polycarbonate filter (3.0 μm pore size; BD Biosciences). DiI was allowed to diffuse overnight at 4°C. The slices were then post-fixed in 4% PFA for 1 hr prior to mounting. Images of the basal dendrites (50–60 μm) of layer V pyramidal neurons in the PrL-C region were collected in the Z-plane and used to create a deconvolved 3-D image. A filament of the dendritic shaft and spines was then created using Imaris XT (Bitplane, Zurich, Switzerland). Dendritic spines were classified into 4 categories (long, mushroom, stubby, or filopodia) based on their length, neck, and head width, where *L* is spine length, *WH* is spine head width, and *WN* is spine neck width. Long spines were identified as having a $L \geq 0.75$ μm and < 3 μm, mushroom spines having a $L < 3.5$ μm, $WH > 0.3$ μm and a $WH > WN$, stubby spines having a $L < 0.75$ μm, and filopodia having a $L \geq 3$ μm. Very few spines were classified as filopodia and were thus excluded from further statistical analyses. Analysis was performed on basal dendrites beginning ~75 μm distal to the soma. Spine data (*N* = 10/group; 75 dendritic sections (2-9 sections/rat); 6875 spines) were averaged for each dendritic section and then analyzed as a mixed linear model (SAS PROC MIXED) in addition to Tukey's post hoc test.

Western blotting

The effects of AIE on expression of a select group of proteins in a membrane-enriched fraction were quantified using standard immunoblot procedures as previously described (Kroener *et al*., 2012). Rats were euthanized by decapitation, the brains rapidly removed and immediately immersed for 1-2 min in ice-cold phosphate buffered saline (pH 7.4). The brain was then sectioned on ice into 1 mm thick coronal slices using an adult rat brain matrix (ASI Instruments, Warren, MI). Punches containing the PrL-C region were obtained from the slices on an ice-cold dissecting plate and the tissue temporarily stored at -80°C. Subsequently, a detergent soluble and detergent resistant membrane fraction was prepared as previously described (Mulholland *et al.*, 2011). An aliquot of each sample was diluted with NuPAGE 4X LDS sample loading buffer (Invitrogen Corp., Carlsbad, CA; pH 8.5) containing 500 mM dithiothreitol, and samples were denatured for 10 min at 70°C. Five μg of each sample was separated using the Bis-Tris (375 mM resolving buffer and 125 mM stacking buffer, pH 6.4; 7.5% acrylamide) discontinuous buffer system with

MOPS electrophoresis buffer (50 mM MOPS, 50 mM Tris, 0.1% SDS, 1 mM EDTA, pH 7.7). Protein was then transferred to Immobilon-P PVDF membranes (Millipore, Bedford, MA) using a semi-dry transfer apparatus (Bio-Rad Laboratories, Hercules, CA). After transfer, blots were washed with phosphate-buffered saline containing 0.1% Tween 20 (PBST) and then blocked with PBST containing 5% nonfat dried milk (NFDM) for 1 hr at room temperature with agitation. The membranes were then incubated overnight at 4°C with primary antibodies directed against GluN1 (1:4000; BD Transduction Laboratories, San Jose, CA; Catalog # 556308), GluN2A (1:2000; Millipore Corp., Billerica, MA; Catalog # AB07-632), GluN2B (1:2000; NeuroMab, Antibodies, Inc. & UC Davis, Davis, CA; Catalog # 75-097), GluA1 (1:2000; Millipore Corp., Billerica, MA; Catalog # AB1504), GluA2 (NeuroMab, Antibodies, Inc. & UC Davis, Davis, CA; Catalog # 75-002), PSD-95 (1:5000; NeuroMab, Antibodies, Inc. & UC Davis, Davis, CA; Catalog # 75-028) or COMT (1:1000; BD Transduction Laboratories, San Jose, CA; Catalog # 611970) diluted in PBST containing 0.5% NFDM and washed in PBST prior to 1 hr incubation at room temperature with horseradish peroxidase conjugated secondary antibodies diluted 1:2000 in PBST. Membranes received a final wash in PBST and the antigen-antibody complex was detected by enhanced chemiluminescence. The band corresponding to the appropriate sized protein was quantified by mean optical density using computer-assisted densitometry with ImageJ v1.41 (National Institutes of Health, USA). Unpaired Student's *t*-test was used to detect significant differences between control and AIE at each age. Although the use of high-abundance proteins as a loading control to normalize expression has been an accepted method, this approach can introduce additional confounds. For example, recent evidence suggests that high-abundance proteins are not linear in the same range as most proteins of interest, and normalizing to a loading control that is not within the same linear range may introduce an added variable that can skew the results and even increase the rate of false negatives (for example, see Aldridge *et al.*, 2008) and (Dittmer and Dittmer, 2006). Evidence also suggests that normalizing to a total protein stain (e.g. Swift Total Protein Stain) is a more reliable method. However, we have found that any variance of total protein stain in each lane normalizes across multiple experiments and that normalizing to protein stain can introduce an unnecessary variable, and in our hands, relying upon the quantitative aspect of the protein assay used to determine the volume needed for loading equal amounts of protein in each lane is a more

reliable metric. We also have tested for differences in protein transfer across lanes using the Swift Total Protein Stain from many different membranes, and found that total protein stain across lanes did not markedly differ, indicating the amount of protein loaded in the lanes was very consistent.

MB-COMT promoter methylation

The isolated DNA was sonicated to 200 bp fragments and subjected to MethylMiner™ methylated DNA enrichment (Cat. #ME10025, Life Technologies, Carlsbad, CA) also according to the protocol provided by the manufacturer. This method uses MBD-Biotin molecules to pull down methylated fragments. A single high salt (2 M NaCl) elution was then carried out and the resulting DNA amplified by Real-Time quantitative PCR using the RT2 SYBR Green ROX qPCR Mastermix (Cat. #330522, QIAGEN Inc., Valencia, CA). Primers were obtained from IDT (Integrated DNA Technologies Inc., Coralville, Iowa) and were designed to span two important transcriptional control regions in the rat COMT gene. The first primer set is located in the upstream putative promoter region of Exon I and the second spans the upstream and beginning region of Exon II, which contains a CpG site similar to Exon III of human COMT promoter, indicating that this may be a conserved CpG site (Murphy *et al.*, 2005) (Figure 3). Primer sequences for exon I were CCAGAACACTGGTCTCGTGATA (forward) and TGTGGGAGTGTCCACAGG (reverse), and the sequences for Exon II were GAAGGGCACAAGACACACAG (forward) and GGAGACCCAATGAGACTGCA (reverse). Input genomic DNA that was not subjected to the methylation enrichment was used as a control and fold change was calculated using the $2^{-\Delta\Delta CT}$ method (Livak and Schmittgen, 2001).

Electrophysiological Recordings

Rats were anesthetized with isoflurane, and the brain was immediately removed and placed in an ice-cold ACSF dissection solution containing (in mM): 125 NaCl, 2.5 KCl, 1.25 $NaHPO_4$, 25 $NaHCO_3$, 4 $MgCl_2$, 1 $CaCl_2$, 10 d-glucose, 15 sucrose, 0.4 ascorbic acid. Slices were incubated at 34°C for at least 1 hr before recordings in continuously aerated (5% carbon dioxide/95% oxygen) incubation ACSF containing (in mM): 125 NaCl, 2.5 KCl, 1.25 $NaHPO_4$, 25 $NaHCO_3$, 4 $MgCl_2$, 1 $CaCl_2$, 10 d-glucose, 15 sucrose, 0.4 ascorbic

acid, and 2 kynurenic acid. After incubation, slices were transferred to a submerged recording chamber, held at 34°C, and bathed with oxygenated recording ACSF containing (in mM): 125 NaCl, 2.5 KCl, 25 $NaHCO_3$, 2 $CaCl_2$, 1.3 $MgCl_2$, 10 glucose, 0.4 ascorbic acid. The pH of all solutions listed above was adjusted to 7.3 and osmolarity was adjusted to 300 mOsm.

Recordings were made with a Multiclamp 700B amplifier (Axon Instruments, Union City, California), connected to a computer running Axograph X software. All recordings were obtained from pyramidal neurons and fast-spiking interneurons (FSINs) in Layer V of the PrL-C region (Paxinos and Watson, 2005) identified visually with infrared differential interference contrast optics and video microscopy.

For current-clamp experiments, recording electrodes (4-6 MΩ resistance) were filled with a solution containing (in mM): 125 potassium gluconate, 20 KCl, 10 HEPES, 1 EGTA, 2 $MgCl_2$, 2 Na^{2+}-ATP, and 0.3 Tris-GTP, 10 phosphocreatine, 7.3 pH, 285 mOsmols. To analyze firing characteristics and intrinsic properties, 1 second current steps were applied and increased in 20 pA increments from -100 pA until the cell fired 6-8 action potentials. The size of current step needed to evoke at least 6 action potentials varied across cells but fell within the range of 250 to 400 pA. The same current step was used within each cell to compare firing properties during baseline and following bath application of DA agonist. For voltage-clamp experiments, recording electrodes (4-6 MΩ resistance) were filled with a solution containing (in mM): 135 CsCl, 2 $MgCl_2$, 10 HEPES, 1 EGTA, 4 NaCl, 2 NaATP, and 0.3 Tris-GTP, 10 phosphocreatine, 1 QX-314 Cl^-. The pH was adjusted to 7.3 using KOH and osmolarity was measured to be approximately 285 mOsmols. Series resistances (<20 MΩ) and input resistances were continually monitored throughout the experiment via a 1 mV (100 ms) hyperpolarizing pulse. Excitatory postsynaptic currents were evoked using a tungsten bipolar stimulating electrode placed in layer V within 200 μm of the cell being recorded. The stimulating electrode was connected to a Grass S88 stimulator and stimulus isolation unit. An input-output relationship was obtained by varying the intensity of stimulation from an amount that produced no response up to an amount that produced a response of maximal amplitude regardless of further increases in stimulus intensity. The stimulus intensity was then reduced to elicit a response that was approximately 75% of the maximal amplitude, and evoked responses were then measured at holding potentials from -80 mV to +40 mV in 10 mV increments. Evoked NMDA (eNMDA) and evoked AMPA (eAMPA) currents were

elicited by focal electrical stimulation in the presence of 100 μM picrotoxin and either CNQX (10 μM) or dl-APV (50 μM), respectively.

Immunohistochemistry

Expression of TH, D_1 receptors and the norephinephrine transporter (NET) was determined in the PrL-C using standard immunohistochemical procedures. Control and AIE-exposed adult rats were transcardially perfused with PBS (pH 7.4) followed by perfusion with 4% paraformaldehyde. The brain was then rapidly removed from the skull and immediately immersed in 4% paraformaldehyde overnight followed by immersion in 30% sucrose for 48-72 hr. Brains were subsequently frozen and sectioned coronally at 40 μm using a cryostat maintained at -22°C. Free floating sections were stored in cryoprotectant at -20°C until ready for immunohistochemical processing.

To examine TH immunolabeling (performed at University of North Carolina), slices were pretreated with 2% Triton-X for 5 minutes, and incubated with a rabbit polyclonal antibody against TH (1:500, Millipore, AB152) overnight at 4°C. The sections were then rinsed and incubated with a biotinylated goat anti-rabbit for 1 hr at room temperature. The sections were then rinsed and incubated for 1 hr with avidin-biotin complex reagents (Vector ABC kit, Vector Laboratories). Diaminobenzidine (DAB, Sigma) was used as a chromagen to develop the reaction with 0.05% of a 3% stock of H_2O_2 and nickel ammonium sulfate (2.5%, Sigma) was used to enhance the reaction. Each step was separated by three 10 min washes in PBS. Sections were mounted on glass slides and cover-slipped with DPX mounting media. Images were captured using an Olympus BX50 microscope and Sony DXC-390 video camera, and TH immunolabeling quantified using Bioquant Nova Advanced Image Analysis (R&M Biometric, Nashville, TN) as previously described (Liu *et al.*, 2008). For TH positive immunolabeling, the PrL-C region (bregma 3.2 to 2.2 mm (Paxinos and Watson, 2005) were outlined and pixel density measured from the outlined area. From each section, data was obtained from both the left and right hemisphere from at least four to five sections for each brain, and the average value were used and reported as the mean of those sections.

To examine D_1 receptor and NET immunolabeling (performed at Medical University of South Carolina), slices were first rinsed in PBS followed by incubation in 1% H_2O_2 for 1 hr to inhibit endogenous peroxidases. Non-specific binding was blocked by incubation in PBS containing 0.4% Triton-X and 5% normal donkey serum for 1 hr. The tissue was then incubated overnight at room temperature in the same solution with the addition of the primary antibody (D_1: rabbit polyclonal, 1:2000; ADR-001, Alomone Labs, Jerusalem, Israel; NET: mouse monoclonal, 1:3000; NET05-2, MAb Technologies, Stone Mountain, GA) followed by incubation in biotinylated donkey anti-mouse (NET) or anti-rabbit (D_1) secondary antibody (1:1000; Jackson ImmunoResearch, West Grove, PA) for 30 min. The antigen was then visualized by incubation in ABC (Vectastain Elite Kit; Vector Laboratories) for 1 hr followed by incubation in 0.05% 3,3-diaminobenzidine, 0.05% ammonium nickel(II) sulfate hexahydrate and 0.015% H_2O_2 for 20 min. Sections were then mounted on Frost Plus slides, dried, dehydrated, and coverslipped in preparation for analysis. Images were captured at 10X magnification under identical illumination using an infinity plan achromatic compound microscope (AmScope, Irvine, CA). Before acquiring measurements, a flat field correction was performed on each image using the Imaging Calculator Plus plugin in ImageJ to ensure the fidelity of data acquisition across slices. Following flat field correction, optical density of immunolabeling was measured in the PrL-C of both hemispheres across three sections taken from the same approximate level as was used for TH measurements using ImageJ. Measurements within each subject were averaged across hemispheres and across sections to obtain a single measure of staining intensity. Values from one control rat were excluded due to extensive tissue damage during processing.

Supplemental Figure S1

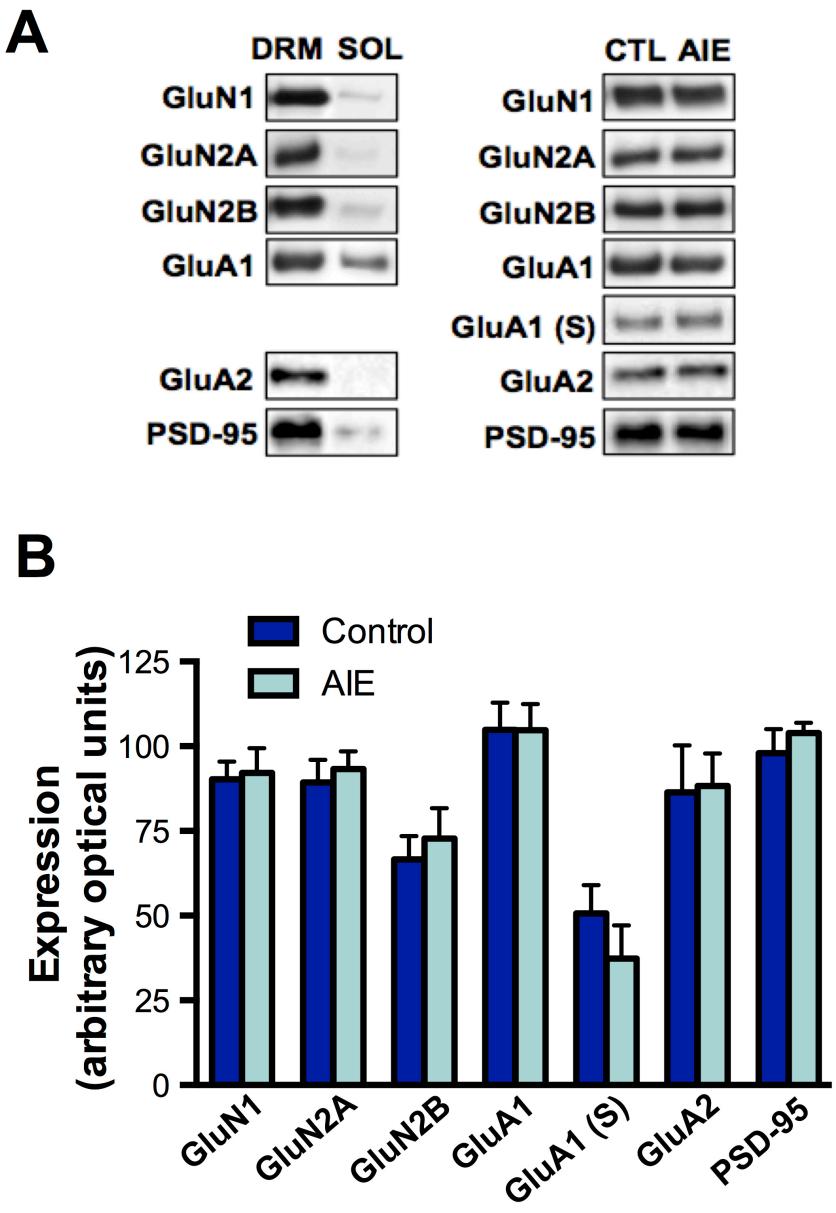

Figure S1. Adolescent intermittent ethanol exposure does not alter glutamate receptor protein expression in the adult mPFC. **(A)** Representative blots of NMDA and AMPA receptor subunits in fractionated tissue from control and AIE-exposed adult rats. (DRM = Triton X-100 resistant fraction, Sol = Triton X-100 soluble fraction). **(B)** AIE has no effect on AMPA or NMDA receptor subunit protein expression in the adult mPFC. Data represents analysis of expression in the DRM with the exception of GluA1, which represent analysis in the DRM and soluble fraction [designated as GluA1(S)] (n = 5-7 rats/group).

Supplemental Figure S2

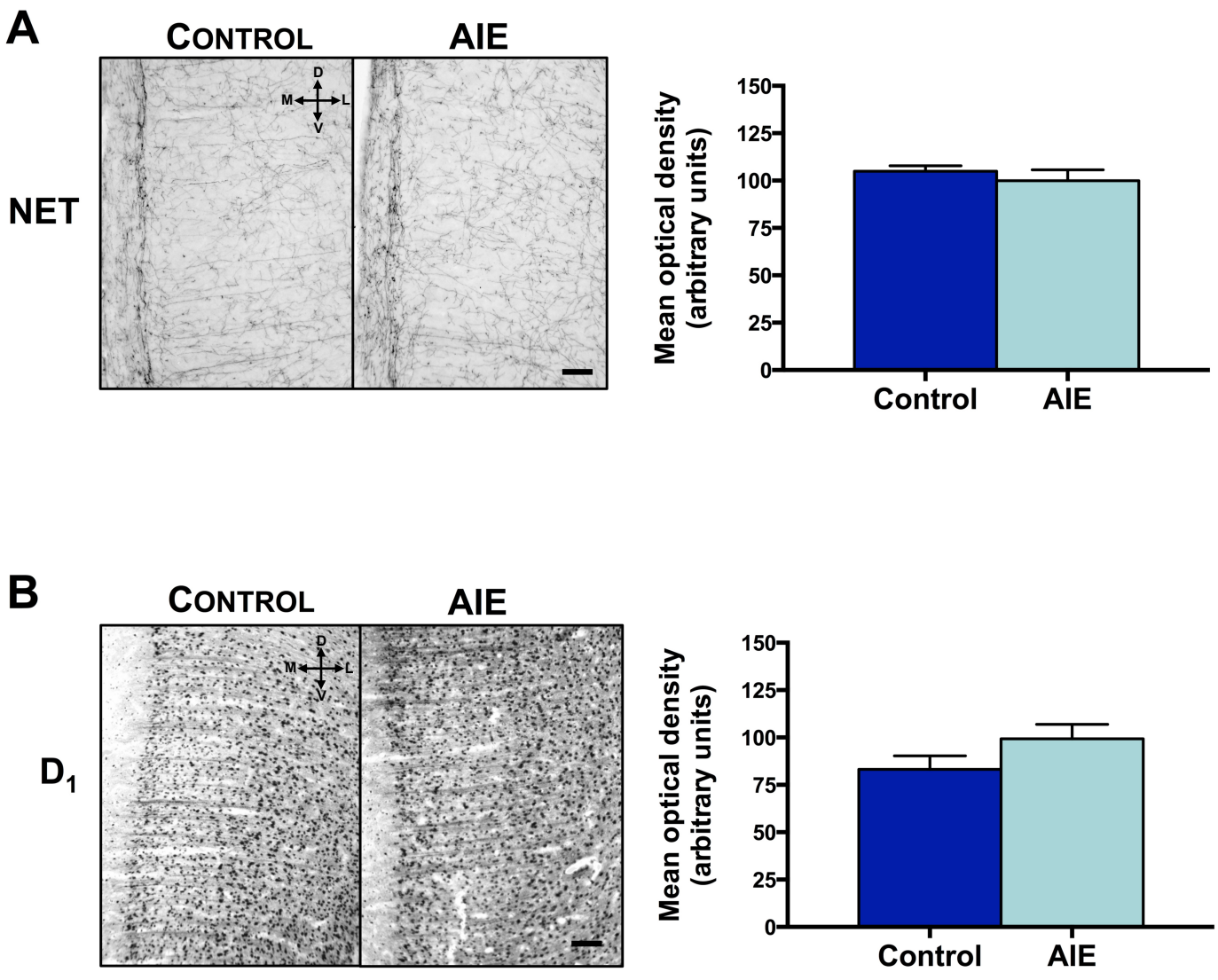

Figure S2. Effect of adolescent intermittent ethanol exposure on NET protein and D_1 receptor expression in the adult PrL-C. **(A)** Shown on the left panel are representative images of the staining of NET in PrL-C slices obtained from control and AIE-exposed adult rats. As shown in the graphs to the right, AIE did not alter the expression of NET compared to controls. **(B)** Shown on the left panel are representative images of the staining of D_1 receptors in PrL-C slices obtained from control and AIE-exposed adult rats. As shown in the graphs to the right, AIE did not alter the expression of D_1 compared to controls. In both A and B,

indicator in upper right corner of photomicrograph shows slice orientation (D-dorsal; L-lateral; V-ventral; M-medial) (control n = 6; AIE: n = 8 rats/group).

Table S1. Measurement of Intoxication and blood ethanol concentrations (BEC)

Cycle	Intox Score Day 1*	Intox Score Day 2*	BEC Measurement Day 2 (mg%)[#]
1	2.53 ± 0.14	2.18 ± 0.14	298.04 ± 14.41
2	2.87 ± 0.16	2.56 ± 0.12	334.41 ± 10.31
3	2.27 ± 0.12	2.16 ± 0.10	299.66 ± 10.39
4	1.91 ± 0.11	1.95 ± 0.09	230.79 ± 11.32
Grand Avg	2.39 ± 0.05	2.21 ± 0.04	290.73 ± 6.10

*Intoxication was scored on a 1-5 rating scale at the end of each 14 hr ethanol vapor exposure period.
[#]Tail-vein blood was drawn at the end of each of the 2-day ethanol vapor exposure cycles.
*[#]All values represent the mean ± sem.

Table S2. Intrinsic properties of pyramidal neurons in layer V of the PrL-C.

Age (postnatal days)	I_h (sag+rebound ADP)*	V_{rest} #	R_{in} (MOhms)&	Evoked FR+ Baseline and post SKF38393	Evoked FR+ Baseline and post quinpirole
Early (P14-21)	2.6 ± 0.5	-65.3 ± 0.9	121.2 ± 8.7	N = 2/8 3.5 ± 0.5 6.5 ± 1.5	N = 4/7 3.3 ± 0.5 1.9 ± 0.4
Middle (P28-P35)	2.8 ± 0.2	-63.4± 0.9	115.7 ± 10.3	N = 5/6 3.6 ± 0.8 5.2 ± 0.8	N = 6/8 3.3 ± 0.4 2.3 ± 0.4
Late (P46-P58)	3.2 ± 0.4	-62.4 ± 0.9	119.4 ± 9.7	N = 5/6 4.6 ± 0.6 6.0 ± 0.6	N = 9/11 4.6 ± 0.7 3.4 ± 0.7
Adult (P100+)	3.3 ± 0.4	-61.8 ± 2.0	128.4 ± 11.2	N = 8/8 3.9 ± 0.7 4.8 ± 0.8	N = 8/8 4.9 ± 0.4 2.1 ± 0.7
Controls	3.2 ± 0.4	-63.6 ± 3.7	123.4 ± 12.6	see Figure 5B	see Figure 5B
AIE	2.7 ± 0.4	-65.1 ± 2.2	118.9 ± 7.9	see Figure 5B	see Figure 5B

*I_h current
#Resting membrane potential (V_{rest})
&Input resistance (R_{in})
+Firing Rate (FR)

Table S3. Intrinsic Properties of fast-spiking neurons in layer V of the PrL-C.

	V_{rest} [#]	AHP[§]	Adaptation ratio[$]	AP amplitude	AP duration (msec)
Controls	-81.2 ± 3.2	14.6 ± 2.3	1.1 ± 0.12	52.6 ± 11.7	0.5 ± 0.12
AIE	-82.6 ± 2.6	15.1 ± 3.6	1.2 ± 0.15	53.8 ± 12.6	0.8 ± 0.09

[#]Resting membrane potential (V_{rest}; in mV)
[§]Afterhyperpolarization
[$]ISI (ratio of the interspike interval (ISI) of first two spikes of current step divided by ISI of last two spikes of same current step)

References

Aldridge, GM, DM Podrebarac, WT Greenough and IJ Weiler (2008). The use of total protein stains as loading controls: an alternative to high-abundance single-protein controls in semi-quantitative immunoblotting. *J Neurosci Methods* **172**(2): 250-254.

Dittmer, A and J Dittmer (2006). Beta-actin is not a reliable loading control in Western blot analysis. *Electrophoresis* **27**(14): 2844-2845.

Gass, JT, WB Glen, Jr., JT McGonigal, H Trantham-Davidson, MF Lopez, PK Randall, et al. (2014). Adolescent alcohol exposure reduces behavioral flexibility, promotes disinhibition, and increases resistance to extinction of ethanol self-administration in adulthood. *Neuropsychopharmacology* **39**(11): 2570-2583.

Kroener, S, PJ Mulholland, NN New, JT Gass, HC Becker and LJ Chandler (2012). Chronic alcohol exposure alters behavioral and synaptic plasticity of the rodent prefrontal cortex. *PLoS One* **7**(5): e37541.

Liu, Y, L Qin, B Wilson, X Wu, L Qian, AC Granholm, et al. (2008). Endotoxin induces a delayed loss of TH-IR neurons in substantia nigra and motor behavioral deficits. *Neurotoxicology* **29**(5): 864-870.

Livak, KJ and TD Schmittgen (2001). Analysis of relative gene expression data using real-time quantitative PCR and the 2(-Delta Delta C(T)) Method. *Methods* **25**(4): 402-408.

Mulholland, PJ, HC Becker, JJ Woodward and LJ Chandler (2011). Small conductance calcium-activated potassium type 2 channels regulate alcohol-associated plasticity of glutamatergic synapses. *Biol Psychiatry* **69**(7): 625-632.

Murphy, BC, RL O'Reilly and SM Singh (2005). Site-specific cytosine methylation in S-COMT promoter in 31 brain regions with implications for studies involving schizophrenia. *Am J Med Genet B Neuropsychiatr Genet* **133B**(1): 37-42.

Paxinos, G and C Watson (2005). The rat brain in stereotaxic coordinates.